

## Structures and Vibrational Spectra of CH<sub>3</sub>OCH<sub>2</sub>CH<sub>2</sub>OH: The Hydrogen-bonded Conformers

Francisco P. S. C. Gil,† R. Fausto, A. M. Amorim da Costa and J. J. C. Teixeira-Dias\*  
 Department of Chemistry, University of Coimbra, P-3049 Coimbra, Portugal

*Ab initio* calculations at the MP2/6-31G\* and MP2/6-31G\*//6-31G\* levels have been carried out for the monomer of 2-methoxyethanol (CH<sub>3</sub>OCH<sub>2</sub>CH<sub>2</sub>OH). The MP2/6-31G\* results indicate that the two more stable conformers (*tGg'* and *gGg'*) display intramolecular hydrogen bonds directed from the hydroxy H atom to one of the lone pairs of the ether O atom, and that the *tGg'* conformer is 6.3 kJ mol<sup>-1</sup> more stable than the *gGg'* conformer. As the MP2/6-31G\* and MP2/6-31G\*//6-31G\* calculations do not yield results differing by more than a few tenths of a kJ mol<sup>-1</sup>, it is concluded that the structure-sensitive and the dynamic correlation corrections are far from being additive. While the optimization of geometry for the correlated wavefunction generally leads to increase of bond lengths and reduction of bond angles, on the whole the geometrical parameters undergo similar changes in different conformers. *Ab initio* harmonic 6-31G\* derived force fields were used to perform normal mode analyses for the more stable conformers. The calculated  $\nu(\text{CH})$  frequencies are found to correlate linearly with some of the *ab initio* calculated CH bond lengths. An interpretation of the FTIR and Raman spectra for the liquid phase consonant with the structural and vibrational *ab initio* results is presented. Two spectral features observed both in Raman and in FTIR spectra and associated with  $\nu(\text{OH})$  in monomeric species are ascribed to conformers, in accord with the theoretical and experimental results. On the whole, both the structural and the vibrational results presented point to a distinction between the hydrogen-bonded *G*-type conformers (*tGg'* and *gGg'*) and the higher energy *T*-type conformers (*tTg* and *tTt*).

Compounds with the general formula C<sub>m</sub>H<sub>2m+1</sub>(OCH<sub>2</sub>CH<sub>2</sub>)<sub>n</sub>OH, abbreviated C<sub>m</sub>E<sub>n</sub>, display a wide range of interesting molecular properties and aggregation patterns in solution<sup>1–18</sup> with important pharmaceutical and industrial applications. On the whole, these properties result from a subtle interplay between the conformational degrees of freedom, the possibility of intramolecular hydrogen bonding, and the relative importance of the polar and non-polar fragments in the extent of intermolecular interactions especially of the hydrogen-bonding type. While C<sub>m</sub>E<sub>n</sub> compounds have been widely studied by different spectroscopic and thermodynamic techniques, an assessment of the relative importance of conformational effects and hydrogen-bond interactions at the unimolecular level is still lacking, though it is of fundamental importance for the understanding of the properties of these compounds at the oligomer level and of their aggregation patterns in solution.

In this work, the structures and relevant conformations of C<sub>1</sub>E<sub>1</sub> (CH<sub>3</sub>OCH<sub>2</sub>CH<sub>2</sub>OH) are determined by *ab initio* MO calculations at the MP2/6-31G\* level. *Ab initio* harmonic 6-31G\* derived force fields are used to perform normal mode analyses for the more stable conformers. The structural and vibrational *ab initio* results are discussed in the light of Raman and FTIR spectra for the liquid phase, and of concentration and temperature variation spectroscopic studies for the  $\nu(\text{OH})$  region.

### Computational and Experimental Methods

*Ab initio* calculations at the MP2/6-31G\* and MP2/6-31G\*//6-31G\* levels were carried out with the GAUSSIAN 92 program system<sup>19</sup> adapted to VAX computers. The absolute errors in bond lengths and bond angles with respect to the equilibrium geometrical parameters are less than 1 pm and 0.1°, respectively, and the stopping criterion for the SCF iterative process required a density matrix convergence of less than 10<sup>-8</sup>.

Normal-coordinate analyses were performed<sup>20</sup> using the *ab initio* derived force fields. While correlated wave functions at the MP2/6-31G\* level were used for the determination of structures and energies, the less expensive and more tractable 6-31G\* basis set was used for the evaluation of the force fields at reference geometries obtained with the same basis set.<sup>21</sup>

Local C<sub>s</sub> symmetry internal coordinates were used throughout. As the calculated frequencies *vs.* observed frequencies yielded a straight line with a high correlation coefficient (0.998 87), the calculated frequencies of the most stable conformer were appropriately scaled [ $\nu_{\text{scaled}} = 0.9123 \times \nu_{\text{calc}} - 72.5$ ]. On the whole, 26 frequency values were used. The mean error in this scaling was 0.5%, and the largest error which occurred in some low-frequency modes did not exceed 17%. Modes which were doubtfully assigned or could not be observed were excluded from the linear regression. The same frequency scaling was assumed for the less stable conformers.

Fig. 1 represents schematically the four more relevant conformations of C<sub>1</sub>E<sub>1</sub>, numbers the atoms, and identifies the conformations. For the identification of the atoms in structural parameters and whenever ambiguity does not occur, the numbers of the atoms are omitted and a left-to-right order of the underlined atomic symbols in C(H<sub>3</sub>)OC(H<sub>2</sub>)C(H<sub>2</sub>)OH is adopted. The optimized geometries of C<sub>1</sub>E<sub>1</sub> are identified by a three-letter acronym specifying the CO—CC (lower case), OC—CO (upper case) and CC—OH (lower case) axes as *trans* (*t*, *T*), + *gauche* (*g*, *G*) or – *gauche* (*g'*, *G'*) arrangements.

2-Methoxyethanol was obtained from Aldrich. Samples of the pure compound and dilute solutions in CCl<sub>4</sub> were prepared.

IR spectra were recorded on a Nicolet FTIR 740 spectrometer, equipped for the 4000–400 cm<sup>-1</sup> region with a germanium on CsI beam splitter and with a DTGS detector with CsI windows. Temperature variation was carried out using a variable-temperature AgCl cell (accuracy to ± 1 K).

Raman spectra were recorded on a triple monochromator Jobin-Yvon T 64000 Raman system (focal distance 0.640 m, aperture *f*/7.5). The pre-monochromator stage was used in the

† Department of Physics.

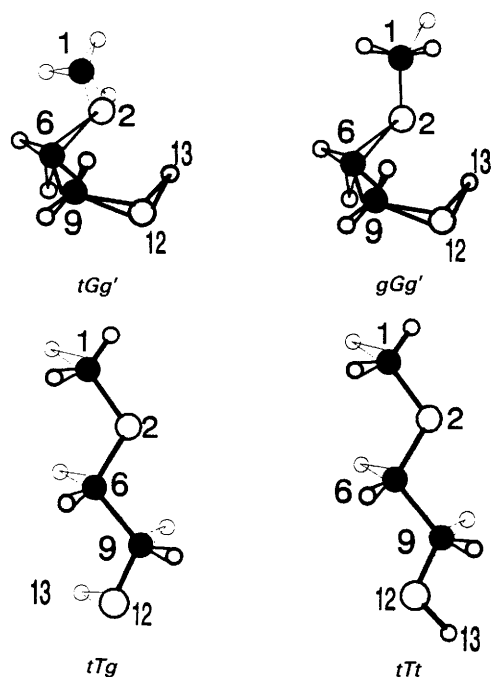


Fig. 1 Numbering of atoms for the four more stable conformations of  $C_1E_1$  (schematic)

subtractive mode. The system is equipped with holographic gratings corrected for aberration ( $1800 \text{ grooves mm}^{-1}$ ), a thermoelectrically cooled photomultiplier and a non-intensified CCD, for optional mono- and multi-channel detection, respectively. The 514.5 nm line of an argon laser (Coherent, model Innova 300-05) was used as excitation radiation. Under the experimental conditions used, the estimated frequency errors were approximately  $\pm 1 \text{ cm}^{-1}$ .

## Results and Discussion

### Energies and Geometries

Table 1 presents the relative conformational energies and dipole moments, and the most relevant optimized structural parameters for the four more stable forms, calculated at the MP2/6-31G\* level. The order of conformational energies is the following:  $tGg' < gGg' < tTg < tTt$ . As can be seen,  $tGg'$  and  $gGg'$  are the two more stable conformers and  $tGg'$  is

the most stable conformer, in agreement with previous calculations.<sup>10</sup> Consideration of the short non-bonded atom  $O \cdots O(H)$  and  $O \cdots H(O)$  distances (Table 1) suggests the occurrence of intramolecular hydrogen bonds in the  $tGg'$  and  $gGg'$  conformers, between the ether O atom and the hydroxy H atom. These intramolecular interactions seem to be decisive to explain the greater stability of these conformers, since the non-hydrogen bonded G-type conformers  $g'Gt$ ,  $tGt$ , and  $tGg$  are less stable than the T-type conformers  $tTg$  and  $tTt$ .

Model comparison of the  $tGg'$  and  $gGg'$  structures suggests that the repulsive interaction between one of the methyl H atoms and one of the H atoms in the methylene group bonded to the alcohol O atom should be mainly responsible for the higher energy of the  $gGg'$  conformer. One important consequence of this repulsive interaction is the opening of the OCC angle in the  $gGg'$  conformer by  $4.3^\circ$  with respect to its value in the most stable conformer (Table 1).

The stabilization effect of correlation increases with the number of *gauche* arrangements along the series  $tTt < tTg < tGg' < gGg'$ , being largest for  $gGg'$  (Table 1). This order seems to indicate that the effect of electrons avoiding each other is less important for *trans* arrangements which tend to keep the lone pairs of distinct O atoms and the H atoms bonded to different atoms further apart. Considering the various *trans*  $\rightarrow$  *gauche* transitions involving the studied conformers, the stabilization energy ( $\text{kJ mol}^{-1}$ ) increases in the following order:  $\text{CO}-\text{CC}$  ( $tGg' \rightarrow gGg' = 3.3$ )  $<$   $\text{OC}-\text{CO}$  ( $tTg \rightarrow tGg' = 5.3$ )  $<$   $\text{CC}-\text{OH}$  ( $tTt \rightarrow tTg = 8.7$ ). These correlation corrections are of the same magnitude, or in some cases larger than, conformational energy differences and change appreciably with the conformational transition considered. This stresses the importance of including correlation whenever conformational energy differences in this type of molecules are evaluated. In addition, since these correlation corrections reach their largest value for the *trans*  $\rightarrow$  *gauche* transition in the  $\text{CC}-\text{OH}$  axis, it is concluded that correlation is also of great importance to account adequately for the energetics of hydrogen-bond formation.

Comparison of the MP2/6-31G\* and MP2/6-31G\*\*/6-31G\* results enables us to assess the extent of the structure-sensitive correlation correction, as the first calculation includes geometry optimization at the MP2 level and the second uses the 6-31G\* optimized geometries. As far as conformational energy differences are concerned, these two cal-

Table 1 Relevant MP2/6-31G\* results for the more stable conformers of  $C_1E_1$

conformer	$tGg'$	$gGg'$	$tTg$	$tTt$
CO-CC; OC-CO; CC-OH/degrees	-173; 60; -50	82; 54; -42	-178; 180; 72	180; 180; 180
$E/E_h^a$	-268.7004112	-268.6980241	-268.6948941	-268.6948569
$\Delta E^b$	0.0	6.3	14.5	14.6
$\Delta E_{\text{correlation}}^{b,c}$	0.0	-3.3	5.3	14.0
$\mu/D^d$	2.86	2.87	2.35	0.32
bond lengths/pm <sup>e</sup>				
C-O	142.0	142.4	141.8	141.7
O-C	142.4	143.1	141.7	141.8
C-C	151.3	151.9	151.8	151.3
C-O	142.1	142.1	142.7	142.7
O-H	97.4	97.5	97.2	97.1
bond angles/degrees <sup>e</sup>				
O-C-C	105.8	110.1	107.4	107.1
C-C-O	110.4	109.8	111.1	106.3
C-O-H	104.6	104.6	107.3	107.6
non-bonded atom distances/pm				
$O \cdots O(-H)$	275.1	277.6	363.8	358.4
$O \cdots H(-O)$	225.1	221.8	392.1	429.4

<sup>a</sup>  $E_h = 2625.5 \text{ kJ mol}^{-1}$ . <sup>b</sup> Energies in  $\text{kJ mol}^{-1}$ ;  $\Delta E = E(\text{conformer}) - E(tGg')$ . <sup>c</sup> For  $tGg'$ ,  $E_{\text{correlation}} = -1966.2 \text{ kJ mol}^{-1}$ . <sup>d</sup>  $D = 3.33564 \times 10^{-30} \text{ C m}$ . <sup>e</sup> For identification of the atoms, a left-to-right order in  $\text{C}(\text{H}_3)\text{OC}(\text{H}_2)\text{C}(\text{H}_2)\text{OH}$  is followed.

Table 2 Vibrational spectra and PED, for relevant conformations of C<sub>1</sub>E<sub>1</sub><sup>a</sup>

description	R (liq)	IR (liq)	freq. n-sc. (sc.)	intensity		PED (%) <sup>b</sup>	intensity		PED (%) <sup>b</sup>
				Raman	IR		Raman	IR	
				tGg'				gGg'	
1 ν(OH)	3608 <sup>c</sup>	3607 <sup>c</sup>	4097 (3665)	43	57	1 [100]	42	56	1 [100]
2 ν(CH <sub>3</sub> as.A)	2988	2980	3307 (2944)	89	46	2 [89]	93	43	2 [89]
3 ν(C(9)H as.)	2952	—	3278 (2918)	88	61	3 [76] + 6[22]	93	44	3 [57] + 6[29] + 5[12]
4 ν(CH <sub>3</sub> as.A <sup>n</sup> )	2935	2931	3232 (2876)	61	99	4 [99]	55	79	4 [98]
5 ν(C(6)H as.)	2897	2895	3221 (2866)	23	103	5 [73] + 6[21]	68	71	5 [64] + 8[21] + 3[11]
6 ν(C(9)H s.)	2884	2882	3199 (2846)	168	11	6 [52] + 5[20]	29	13	6 [49] + 7[26] + 3[22]
7 ν(CH <sub>3</sub> s.)	2834	2828	3186 (2834)	127	84	7 [65] + 8[22]	42	60	7 [46] + 8[26] + 6[12] + 5[10]
8 ν(C(6)H s.)	2780	—	3172 (2821)	9	28	8 [70] + 7[25]	177	89	8 [52] + 7[19] + 5[12]
9 δ(C(6)H <sub>2</sub> )	1477	1472	1674 (1455)	10	1	9 [60] + 13[18] + 11[12]	16	4	9 [64] + 11[18] + 13[11]
10 δ(C(9)H <sub>2</sub> )	1457	1456	1660 (1442)	14	2	10 [89] + 11[11]	8	2	10 [78] + 13[12]
11 δ(CH <sub>3</sub> as.A)	—	—	1654 (1436)	5	8	11 [62] + 9[19] + 10[13]	6	5	11 [59] + 13[12]
12 δ(CH <sub>3</sub> as.A <sup>n</sup> )	1413	1408	1645 (1428)	18	5	12 [101]	18	3	12 [86]
13 δ(CH <sub>3</sub> s.)	1376	1369	1634 (1418)	11	5	13 [77] + 9[15]	11	2	13 [64] + 9[29]
14 ω(C(9)H <sub>2</sub> )	—	1326	1596 (1384)	4	42	14 [45] + 15[29] + 25[15]	3	54	14 [58] + 15[18] + 16[14] + 25[12]
15 ω(C(6)H <sub>2</sub> )	1287	—	1551 (1342)	2	65	15 [54] + 14[30]	2	46	15 [72] + 14[16]
16 δ(COH)	1243	1233	1515 (1310)	11	14	16 [32] + 19[28] + 14[17]	12	9	16 [30] + 19[24] + 14[16] + 17[10]
17 ν(C(6)H <sub>2</sub> )	1199	1194	1398 (1203)	9	27	17 [59]	7	34	17 [58]
18 ν(CH <sub>3</sub> A)	1160	1157	1383 (1189)	5	37	18 [31] + 17[21] + 24[16] + 19[15]	1359 (1167)	87	18 [52] + 24[26]
19 ν(C(9)H <sub>2</sub> )	1129	1124	1322 (1134)	4	101	19 [28] + 16[16] + 21[16] + 18[16] + 24[12]	1332 (1143)	28	19 [42] + 16[27]
20 ν(CH <sub>3</sub> A <sup>n</sup> )	1095	—	1300 (1113)	6	5	20 [85]	1298 (1112)	4	20 [85]
21 ν(C(1)—O(2))	1072	1066	1284 (1099)	7	93	21 [46] + 18[21] + 24[15]	1279 (1094)	4	21 [21] + 23[20] + 24[12] + 22[11]
22 ν(C(6)H <sub>2</sub> )	1048	—	1242 (1061)	3	15	22 [37] + 23[36] + 26[13]	1214 (1035)	4	22 [27] + 18[17] + 26[14] + 24[12] + 25[11]
23 ν(C(9)—O(12))	1022	1017	1200 (1022)	2	127	23 [38] + 25[18] + 26[14] + 16[13]	1206 (1028)	4	23 [60] + 16[14]
24 ν(O(2)—C(6))	971	963	1129 (957)	5	17	24 [28] + 21[22] + 26[12]	1097 (928)	8	24 [33] + 26[24] + 24[20]
25 ν(C—C)	895	891	991 (832)	6	12	25 [31] + 22[27] + 23[22]	969 (812)	7	25 [35] + 22[27] + 23[20]
26 ν(C(9)H <sub>2</sub> )	839	833	925 (771)	9	25	26 [39] + 24[28] + 25[13]	911 (759)	9	26 [33] + 26[24] + 25[18] + 21[12]
27 δ(CCO)	545	539	590 (466)	2	10	27 [38] + 30[22] + 22[11] + 29[10] + 26[10]	571 (448)	1	27 [30] + 27[39] + 26[17] + 22[13]
28 τ(CCOH)	—	—	448 (336)	3	166	28 [96]	439 (328)	2	28 [93]
29 δ(COC)	—	—	395 (288)	1	10	29 [45] + 27[32]	468 (354)	<1	8 29 [65]
30 δ(OCC)	—	—	296 (198)	<1	5	30 [39] + 29[30] + 32[27]	320 (219)	<1	12 27 [38] + 30[36] + 29[12]
31 τ(HCO)	—	—	239 (146)	<1	7	31 [76] + 30[10]	217 (125)	6	7 31 [45] + 32[23] + 33[16]
32 τ(OCCO)	—	—	158 (72)	<1	5	32 [81] + 30[13] + 31[17] + 28[11]	151 (65)	<1	5 32 [66] + 31[37] + 30[21] + 28[11]
33 τ(COCC)	—	—	99 (18)	<1	2	33 [99]	79 (73)	<1	1 33 [119] + 32[28] + 31[26] + 28[19]

<sup>a</sup> Frequencies in cm<sup>-1</sup>; n-sc. = non-scaled; sc. = scaled; for the frequency scaling see 'Experimental and Computational Methods'; ν, stretching; δ, bending; w, wagging; γ, rocking; t, twisting; τ, torsion; s, symmetric; as, asymmetric. <sup>b</sup> PED values smaller than 10% are not shown. <sup>c</sup> Values obtained in diluted solutions in CCl<sub>4</sub>.

culations do not yield results differing by more than a few tenths of a  $\text{kJ mol}^{-1}$ . This leads us to conclude that the correlation correction at the MP2/6-31G\*//6-31G\* level accounts also for the energy change which results from geometry optimization at the MP2/6-31G\* level, *i.e.* the structure-sensitive and the dynamic correlation corrections are far from being additive. In addition, from the small changes of the conformational energy differences obtained by these two types of calculations, it can be concluded that the geometry optimization carried out with the correlated wave function tends to stabilize the intramolecular hydrogen bond, since it increases slightly the energy separation between the hydrogen bonded *G*-type conformers (*tGg'* and *gGg'*) and the *T*-type conformers (*tTg* and *tTt*).

Considering now the geometrical parameters in both calculations, it is concluded that the optimization of geometry for the correlated wave function leads, in general, to an increase of bond lengths and a reduction of bond angles, following a previously mentioned trend which improves general agreement of the absolute values with experimental data.<sup>22,23</sup> However, on the whole, the geometrical parameters undergo similar changes in different conformers. This observation is of great practical importance, as it indicates that the more time-consuming and expensive geometry optimization carried out at the MP2 level is not strictly necessary to evaluate changes in the geometrical parameters which are conformationally induced. Based on this conclusion we will obtain geometrical parameters profiles along different dihedral coordinates and force fields for different conformers using, in both cases, 6-31G\* optimized geometries.

At room temperature, approximately 92% of the molecular population should have the *tGg'* conformation, leading us to expect that this is the most dominant form in the gaseous phase at sufficiently low pressures or in very dilute solutions in inert solvents, when both oligomer formation and aggregation in general are not likely to occur. By contrast, the single symmetric form among those studied herein, *i.e.* the all-*trans* conformer, besides having an energy much higher than that of the *tGg'* conformer ( $14.6 \text{ kJ mol}^{-1}$ ), presents also a very small dipole moment (0.32 D), in fact, the smallest dipole moment among the considered conformers (Table 1). Hence, dipole-dipole non-specific intermolecular interactions like those which are expected to occur in diluted solutions of polar aprotic solvents should not contribute much for the stabilization of the symmetric all-*trans* conformer in solution.

In order to characterize the most important intramolecular interactions in the various conformers, the conformational dependence of some relevant structural parameters (Table 1) is now considered and discussed.

Starting with the more stable form (*tGg'*), the most pronounced variations, dihedral angles and  $\text{O}\cdots\text{O}(-\text{H})$  and  $\text{O}\cdots\text{H}(-\text{O})$  distances apart, occur for the CCO angle, which opens by *ca.*  $4^\circ$ , and for the COH angle, which closes by  $3^\circ$ , with respect to the *tTt* form. These variations are consistent with the formation of an intramolecular hydrogen bond ( $\text{O}\cdots\text{H}-\text{O}$ ) in the *tGg'* conformer, as they point clearly towards a more linear  $\text{O}\cdots\text{H}-\text{O}$  axis and a shorter  $\text{O}\cdots\text{H}$  distance (see Table 1). It is interesting to point out that similar changes are observed in the same structural parameters for the *gGg'* conformer, in particular, the CCO angle increases by  $3.6^\circ$  and the COH angle diminishes by  $3^\circ$ . However, if these two conformers (*tGg'* and *gGg'*) are compared (Fig. 1) and the *tGg' → gGg'* transition is considered, the OCC angle opens by *ca.*  $4^\circ$  in the *gGg'* form in order to reduce the steric repulsive interaction in this conformer between one of the methyl H atoms and one of the H atoms in the methylene group bonded to the alcohol O atoms (see Fig. 1). This repulsive interaction in the *gGg'* conformer may

explain the greater stability of the *tGg'* conformer. The *tGg' → gGg'* transition is concomitant with an increase of 2.5 pm in the  $\text{O}\cdots\text{O}(-\text{H})$  distance and a reduction of 3.3 pm in the  $\text{O}\cdots\text{H}(-\text{O})$  distance (Table 1). The latter variation seems to result from the fact that the ether O atom becomes more in line with the H—O bond in the *gGg'* conformer than in the *tGg'* conformer, as the C—O and O—C bonds increase slightly in the *gGg'* conformer. Finally, for the *tTg* form, the most pronounced geometrical change with respect to the *tTt* conformer occurs for the CCO angle which is *ca.*  $5^\circ$  larger in the *tTg* form in order to reduce a repulsive steric interaction between the hydroxy H atom and one of the H atoms in the methylene group bonded to the ether O atom (see Fig. 1).

In conclusion, the OCC, CCO, and COH bond angles are very sensitive to different conformational changes due to internal rotations about the CO—CC, CC—OH and OC—CO axes, respectively.

### Vibrational Frequencies

In this section, the 6-31G\* derived force field is used to calculate the frequencies, the potential-energy distribution (PED), and the IR and Raman intensities of the more relevant conformers. Emphasis is given to the modes which exhibit large sensitivities, in frequency and/or composition, to conformational changes. Table 2 presents the vibrational calculated results for the *tGg'* and *gGg'* conformers.

The occurrence of two 'windows' at *ca.* 2700–1500 and 800–600  $\text{cm}^{-1}$ , both in the calculated and experimental Raman and IR spectra of  $\text{C}_1\text{E}_1$ , immediately suggests the consideration of three spectral regions for the discussion of the vibrational spectra: 3700–2700  $\text{cm}^{-1}$ , 1500–800  $\text{cm}^{-1}$ , and below 600  $\text{cm}^{-1}$ . However, since the OH stretching is particularly sensitive to aggregation which, in turn, should not be involved in the discussion of the conformational degrees of freedom of the monomer for clarity of this text, the  $\nu(\text{OH})$  region will be separately considered at the end of this section in a 'spectral region' of its own.

For sufficiently diluted solutions in  $\text{CCl}_4$ , the occurrence of two IR spectral features associated with  $\nu(\text{OH})$  in monomeric species is now well established.<sup>1,2,4,7,8,13–16</sup> With the exception of this spectral region, the number of intense (*vs*, *s*, and *m*) and well defined bands in the spectra of the liquid at room temperature does not exceed the total number of distinct frequencies expected for the fundamental vibrations of a single conformer ( $3N - 6 = 33$ ). This observation is consonant with the large population calculated for the most stable conformer at room temperature (92%). Hence, only the frequencies of the relatively intense Raman and IR bands of the pure liquid (Fig. 2) and the calculated frequencies for the most stable conformer were considered in the  $\nu_{\text{exp}}$  vs.  $\nu_{\text{calc}}$  linear regression.

### 3200–2700 $\text{cm}^{-1}$ Region

This region includes the  $\nu(\text{CH}_2)$  and  $\nu(\text{CH}_3)$  vibrations which correspond, for a single molecule, to seven CH oscillators and as many distinct frequencies since no degeneracies occur. The four highest frequencies should be ascribed to the anti-symmetric modes (two for the  $\text{CH}_3$  group, one for each  $\text{CH}_2$  group), the lowest three frequencies should correspond to the symmetric modes. This expected general pattern is observed for the *tGg'*, *gGg'* and *tTt* conformers.

The antisymmetric components of the  $\text{CH}_2$  groups, in particular of  $(\text{O})\text{CH}_2$ , change appreciably, both in frequency and composition, with conformation. Both  $\nu(\text{CH}_3 \text{ as } A')$  and  $\nu(\text{CH}_3 \text{ as } A'')$  calculated non-scaled frequencies increase with the number of *gauche* arrangements along the series  $tTt < tTg < tGg' < gGg'$ . In addition, these frequencies ( $\text{cm}^{-1}$ ) present reasonable linear correlations with methyl CH

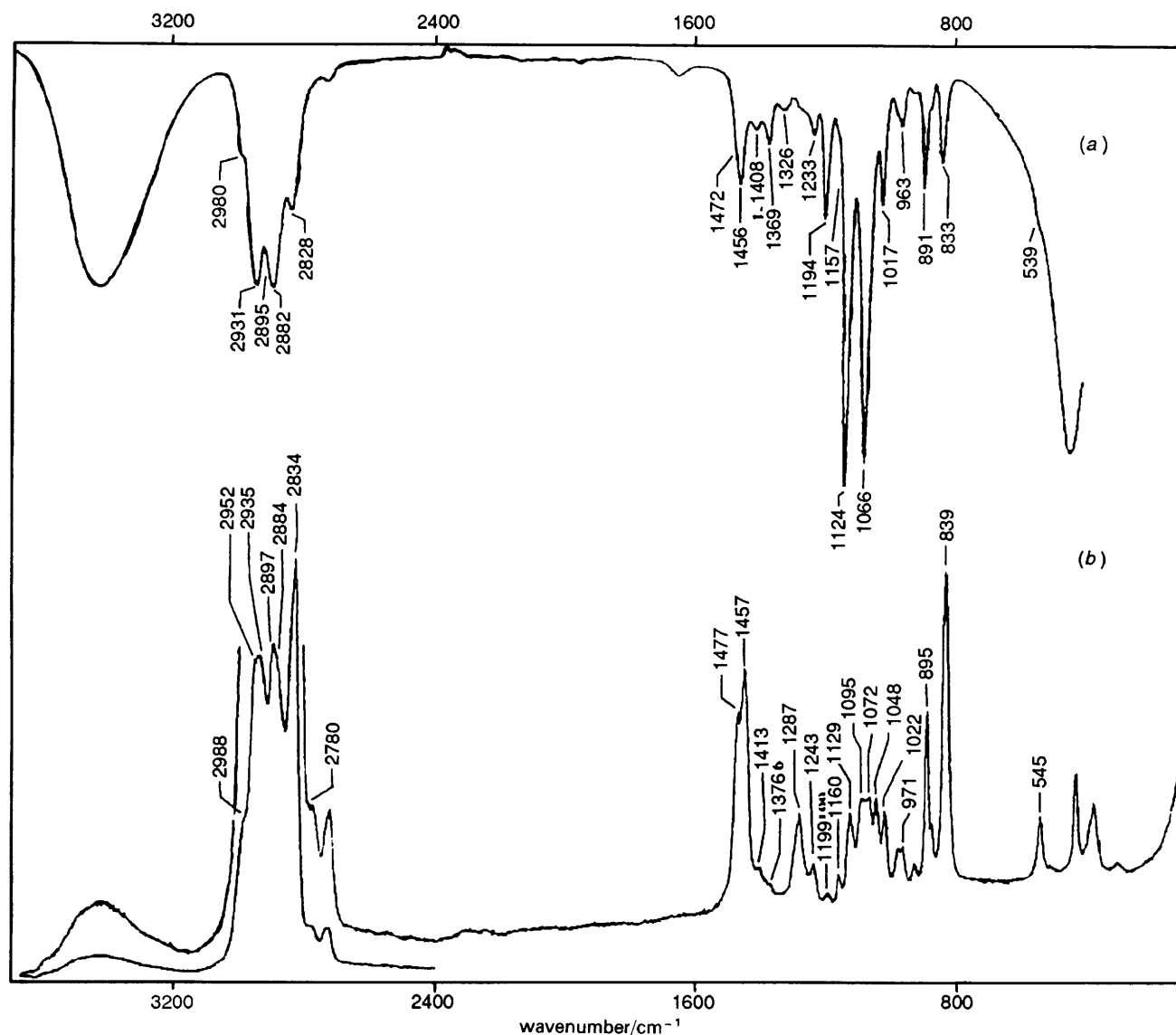


Fig. 2 (a) FTIR and (b) Raman spectra of 2-methoxyethanol (pure liquid, room temperature)

bond lengths (pm):  $\nu(A') = -134.99r(C_1H_3) + 17537$  (correlation coefficient  $R^2 = 0.892$ );  $\nu(A'') = -100.54r(C_1H_4) + 13812$  ( $R^2 = 0.973$ ). Hence, it can be concluded that the methyl CH bond lengths, in particular  $r(C_1H_3)$  and  $r(C_1H_4)$ , are appreciably sensitive to conformation. For isolated CH stretching vibrations of alkanes, good linear correlations of  $\nu(CH)$  against  $r(CH)$  have already been considered.<sup>24</sup>

#### 1500–800 $\text{cm}^{-1}$ Region

This region includes the  $\text{CH}_3$  and  $\text{CH}_2$  bending vibrations, the CC and CO stretching modes, and the COH bending vibration, corresponding to a total of 18 fundamental vibrations in the monomer. In particular, 14 bending vibrations (5 involving the  $\text{CH}_3$  group, 4 for each  $\text{CH}_2$  group, 1 COH bending), and 4 stretching vibrations (1 CC and 3 CO) are considered in this region.

The modes which exhibit the largest sensitivities, both in frequency and composition, to conformational changes are  $\delta(\text{COH})$ ,  $\nu(\text{OC})$  and  $\nu(\text{CC})$ , as well as the wagging, twisting and rocking vibrations of the  $\text{CH}_2$  groups. In the most stable conformer, an extensive mixture of coordinates occurs for  $\tau\text{CH}_2$ , for the  $\text{CH}_2$  group adjacent to OH. In addition, the calculated  $\delta\text{COH}$  frequency exhibits a decrease of ca. 150  $\text{cm}^{-1}$  on going from the conformations with a *gauche* arrangement in the CC–OH axis (*tGg'*, *gGg'*, *tTg*) to the all-

*trans* conformer. This large frequency shift is consonant with the calculated profile of the COH angle variation *vs.* CC–OH, as discussed above.

#### Region below 600 $\text{cm}^{-1}$

For a single molecule, this region includes a total of seven fundamental vibrations, namely, three skeletal bending vibrations (CCO, COC, OCC) and four torsional modes (COCC, OCCO, CCOH, HCOC).

Among the conformers considered herein, only for the most stable conformer does  $\delta(\text{OCC})$  mix with  $\tau(\text{OCCO})$  and to an appreciable extent (27%). It is interesting to point out that, for *n*-butane, a similar vibrational coupling has been previously observed and discussed between  $\delta(\text{CCC})$  and  $\tau(\text{CCCC})$ , also for the *gauche* conformation.<sup>25</sup>

For  $\tau(\text{COCC})$ ,  $\tau(\text{OCCO})$  and  $\tau(\text{HCOC})$ , the frequency shifts due to conformational changes are larger whenever the conformational coordinate corresponds to the predominant torsional mode involved. Generally speaking,  $\tau(\text{CCOH})$  and  $\tau(\text{COCC})$  are pure modes in all the considered conformers, except for *gGg'*, where  $\tau(\text{COCC})$  mixes appreciably with the remaining torsional coordinates.

For the *tTt* and *tTg* conformers,  $\tau(\text{HCOC})$  does not change appreciably, either in frequency (ca. 150  $\text{cm}^{-1}$ ) or in composition [over 86% of PED is from  $\tau(\text{HCOC})$  and

approximately 12% from  $\tau(\text{OCCO})$ ]. In  $gGg'$ ,  $\tau(\text{HCOC})$  occurs at the lowest frequency value among all the studied conformers,  $125\text{ cm}^{-1}$ , and mixes appreciably with  $\tau(\text{COCC})$  and  $\tau(\text{OCCO})$ . For this all-*gauche* form, an appreciable steric interaction is expected to occur between H atoms of the methyl and of the C(9)-methylene groups. Finally, for  $tGg'$ ,  $\tau(\text{HCOC})$  occurs at  $146\text{ cm}^{-1}$ , with a significant 10% PED element from  $\delta(\text{OCC})$ . On the whole,  $\tau(\text{HCOC})$  is not expected to be particularly sensitive to conformational changes, except through an indirect mechanism, whenever repulsive steric interactions involving at least one of the methyl H atoms occur.

#### $\nu(\text{OH})$ Stretching Region

This region displays various important spectral features, occurring, both in the FTIR spectra (Fig. 3) and in the Raman spectra (Fig. 4). Among these, two are ascribed to monomeric species and occur at *ca.* 3640 (shoulder) and 3608  $\text{cm}^{-1}$  (hereafter referred to as A and B, respectively). In addition, a very wide and convoluted complex of bands, referred to as C, occurs in the range 3550–3200  $\text{cm}^{-1}$ .

Band B is the most sharp feature which becomes progressively more prominent at lowering concentrations of  $\text{C}_1\text{E}_1$  in  $\text{CCl}_4$ , both in the FTIR and Raman spectra. In particular, for a 0.01 mole fraction, the IR peak absorbance of B is twice that of C (Fig. 3). It is interesting to mention that the same approximate ratio of intensities ( $\text{B}/\text{C} \approx 2$ ) is observed, in the Raman spectra (Fig. 4), for a much less dilute solution (0.09 mole fraction in  $\text{CCl}_4$ ). In addition, for the same concentration, the Raman spectrum of feature C clearly shows two maxima at *ca.* 3460 and 3310  $\text{cm}^{-1}$ , probably ascribed to different degrees of aggregation, whereas the same feature C shows a single maximum in the FTIR spectrum.

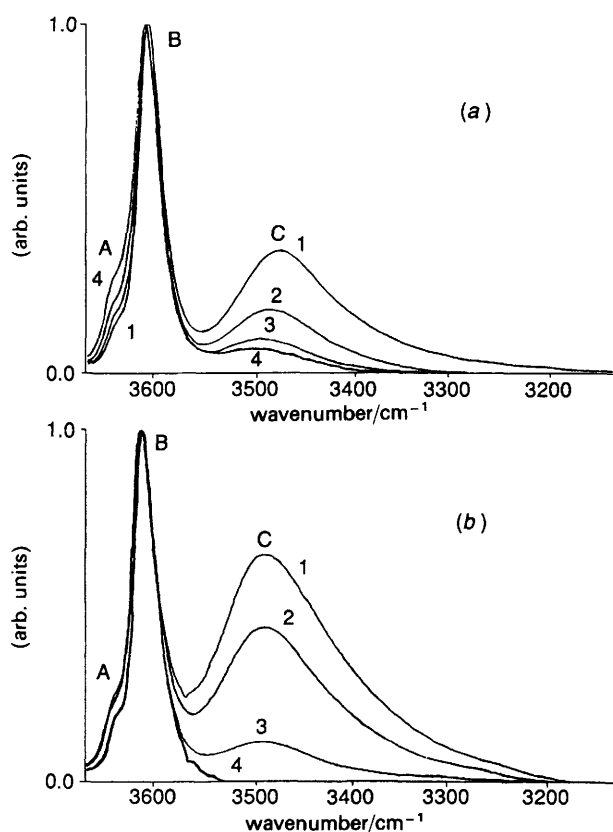


Fig. 3 FTIR spectra of 2-methoxyethanol in  $\text{CCl}_4$  solutions, after smoothing: (a) 0.02 mole fraction solution spectra at 1, 263; 2, 283; 3, 303 and 4, 323 K; (b) room temperature spectra with mole fraction: 1, 0.02; 2, 0.01; 3, 0.002 and 4, 0.0002

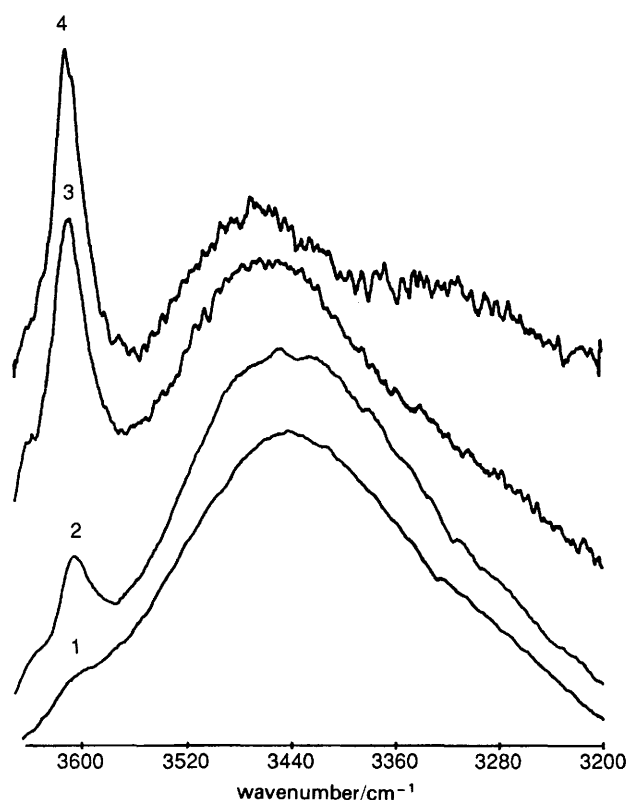


Fig. 4 Raman spectra of 2-methoxyethanol in  $\text{CCl}_4$  solutions at room temperature, after smoothing. Mole fraction: 1, pure liquid; 2, 0.50; 3, 0.17 and 4, 0.09

The absorbance ratio A/B (A is the high-frequency shoulder of B) increases with temperature [Fig. 3(a)], but is relatively insensitive to concentration variation [Fig. 3(b)], at least for the range of concentrations considered (mole fractions varying from 0.02 to 0.0002). By contrast, C is a very broad band whose width increases with concentration, its absorbance and peak frequency being dependent both on temperature and concentration. In particular, the absorbance of C increases and its peak frequency decreases with both reduction in temperature and increase in concentration (Fig. 3).

Previous papers on  $\text{C}_1\text{E}_1$ <sup>1,2,4,7,8,13-16</sup> based their assignments of IR bands A and B on assumptions of the more probable molecular structures, and estimated enthalpy differences from the inverse temperature dependence of the logarithm of the ratio of intensities. To the best of our knowledge, it is the first time that *ab initio* calculations at the levels considered here are used to provide a theoretical and quantitative assessment of the vibrational spectra and to shed light on the interpretation of the above-mentioned spectral features.

The order of the *ab initio* scaled  $\nu(\text{OH})$  frequencies ( $\text{cm}^{-1}$ ) for the various conformers is

$$gGg'(3659) < tGg'(3665) < tTg(3678) < tTt(3690).$$

These results indicate an increase of  $\nu(\text{OH})$  with the number of *trans* arrangements, a trend opposite to that observed for  $\nu(\text{CH}_3)$ . In addition, the hydrogen-bonded conformers ( $tGg'$  and  $gGg'$ ) have close  $\nu(\text{OH})$  scaled frequencies ( $\Delta\nu = 6\text{ cm}^{-1}$ ), a result which suggests the assignment of these conformers to the same observed vibrational band. As expected, the *T*-type conformers have higher  $\nu(\text{OH})$  frequencies than the *G*-type conformers, since the OH oscillators of the latter conformers are intramolecularly hydrogen bonded. It is also interesting to notice that the  $\nu(\text{OH})$  frequency of the all-*trans* conformer

is shifted *ca.* 30 cm<sup>-1</sup> from the centre of the *tGg'*-*gGg'* pair, to higher frequencies. The same approximate frequency difference between bands A and B is observed both in the FTIR (Fig. 3) and Raman spectra (Fig. 4).

The *ab initio* results clearly point to the *tGg'* conformer as the best candidate for band B, since this conformer corresponds to the highest monomer population (92% at room temperature). A small contribution to band B from the *gGg'* conformer is also expected, since the vibrational calculations yield close  $\nu(\text{OH})$  frequencies for the *tGg'* and *gGg'* conformers ( $\Delta\nu = 6 \text{ cm}^{-1}$ ), and the MP2/6-31G\* calculations yield a significant population for the *gGg'* conformer (*ca.* 7%). The proximity of the calculated  $\nu(\text{OH})$  frequencies for the *tGg'* and *gGg'* conformers is not surprising, since the different CO—CC arrangements in these two conformers are not expected to affect the  $\nu(\text{OH})$  frequency appreciably.

For the all-*trans* conformer, the calculated  $\nu(\text{OH})$  frequency is shifted by *ca.* 30 cm<sup>-1</sup> to higher frequencies with respect to the centre of  $\nu(\text{OH})$  for the *G*-type conformers (3662 cm<sup>-1</sup>), in accord with the observed frequency separations between the centres of bands A and B in the FTIR and Raman spectra (*ca.* 32 cm<sup>-1</sup>; Fig. 3 and 4). This agreement points clearly to the *tTt* conformer as the best candidate for band A, though a negligible contribution from the *tTg* conformer should not be totally excluded as this latter conformer is very close in energy to the all-*trans* conformer (Table 1) and the calculated  $\nu(\text{OH})$  frequencies for the *tTt* and *tTg* conformers fall within the observed width of band A. In addition, while the barrier for the *tTt* → *tTg* transition has not been evaluated, it is unlikely to exceed the value of thermal energy ( $RT = 2.5 \text{ kJ mol}^{-1}$  at room temperature), hence providing a mechanism for interconversion between the *tTt* and *tTg* conformers.

The deconvolution of bands A and B is difficult and subject to large errors at least for the weak shoulder, A. However, the relative intensity of this shoulder, A/B, was found to be approximately insensitive to concentration variation in a non-polar solvent (CCl<sub>4</sub>), in agreement with the very low dipole moment of the all-*trans* conformer (Table 1). In addition, from the temperature dependence of the intensities ratio  $I_A/I_B$ , it is possible to estimate a conformational energy difference which falls in the range 7–10 kJ mol<sup>-1</sup>, in accord with the energy difference between the *gGg'* conformer and the *T*-type conformers. This observation gives further support to the above assignment of conformers to bands A and B.

While the calculated intensities should not be considered totally reliable and refer to the isolated molecule as, in fact, all the calculated quantities, it is worth pointing out that the calculated  $\nu(\text{OH})$  Raman intensity for the *tTt* conformer approximately doubles the corresponding intensities for the remaining conformers studied, whereas all the conformers exhibit approximately the same calculated IR line intensities. Apparently, these theoretical results do not agree with experiment, since band A is observed both in the Raman and FTIR spectra. However, as the concentration of C<sub>1</sub>E<sub>1</sub> is progressively reduced, band A becomes clearly distinguishable in the Raman spectra for much less dilute solutions than those which enable observation of the same feature in the FTIR spectra. In fact, for band A to become evident in the FTIR spectra, a more dilute solution (roughly, one tenth of the mole fractions ratio) had to be prepared. These findings lead to the conclusion that the  $\nu(\text{OH})$  band is a more sensitive probe to the presence of monomers in the Raman spectra than in the FTIR spectra.

Since the theoretical results refer to the isolated molecule, care should be exercised in extrapolating the calculated quantities to the liquid-phase spectra, especially to the pure liquid or to concentrated solutions. In particular, the formation of intermolecular hydrogen-bonded oligomers is likely to affect both the geometries and energies of the monomers present in the oligomeric species, hence leading to changes in the observed IR and Raman spectra. Moreover, non-specific intermolecular interactions may also affect the structures and vibrational spectra of monomers. However, both the structural and vibrational results presented herein point to a clear distinction between the hydrogen bonded *G*-type conformers (*tGg'* and *gGg'*) and the higher energy *T*-type conformers (*tTg* and *tTt*).

The authors thank JNICT (Junta Nacional de Investigação Científica), Lisboa, for financial support, and F.P.S.C.G. thanks Instituto Pedro Nunes, Coimbra, for a research grant.

## References

- 1 L. P. Kuhn and R. A. Wires, *J. Am. Chem. Soc.*, 1964, **86**, 2161.
- 2 P. J. Krueger and H. D. Mettee, *J. Mol. Spectrosc.*, 1965, **18**, 131.
- 3 J. Feeney and S. M. Walker, *J. Chem. Soc. A*, 1966, 1148.
- 4 H. Saitō, T. Yonezawa, S. Matsuoka and K. Fukui, *Bull. Chem. Soc. Jpn.*, 1966, **39**, 989.
- 5 R. Iwamoto, *Spectrochim. Acta, Part A*, 1971, **27**, 2385.
- 6 P. Buckley and M. Brochu, *Can. J. Chem.*, 1972, **50**, 1149.
- 7 L. S. Prabhurashi and C. I. Jose, *J. Chem. Soc., Faraday Trans. 1*, 1975, **71**, 1545.
- 8 L. S. Prabhurashi and C. I. Jose, *J. Chem. Soc., Faraday Trans. 2*, 1976, **72**, 1721.
- 9 G. Roux, G. Perron and J. E. Desnoyers, *J. Solution Chem.*, 1978, **7**, 639.
- 10 S. Vázquez, R. A. Mosquera, M. A. Rios and C. Van Alsenoy, *J. Mol. Struct. (Theochem)*, 1989, **188**, 95.
- 11 G. Douhéret, A. Pal and M. I. Davis, *J. Chem. Soc., Faraday Trans. 1*, 1989, **85**, 2723.
- 12 G. Douhéret, A. Pal and M. I. Davis, *J. Chem. Thermodyn.*, 1990, **22**, 99.
- 13 I. Suryanarayana, G. P. Someswar and B. Subrahmanyam, *Z. Phys. Chem.*, 1990, **271**, 621.
- 14 F. A. J. Singelenberg and J. H. Van der Maas, *J. Mol. Struct.*, 1991, **243**, 111.
- 15 F. A. J. Singelenberg, E. T. G. Lutz and J. H. Van der Maas, *J. Mol. Struct.*, 1991, **245**, 173.
- 16 F. A. J. Singelenberg, J. H. Van der Maas and L. M. J. Kroon-Batenburg, *J. Mol. Struct.*, 1991, **245**, 183.
- 17 G. Douhéret and M. I. Davis, *Chem. Soc. Rev.*, 1993, **22**, 43.
- 18 M. I. Davis, *Chem. Soc. Rev.*, 1993, **22**, 127.
- 19 M. J. Frisch, G. W. Trucks, M. Head-Gordon, P. M. W. Gill, M. W. Wong, J. B. Foresman, B. G. Johnson, H. B. Schlegel, M. A. Robb, E. S. Replogle, R. Gomperts, J. L. Anders, K. Raghavachari, J. S. Binkley, C. Gonzalez, R. L. Martin, D. J. Fox, D. J. Defrees, J. Baker, J. J. P. Stewart and J. A. Pople, GAUSSIAN 92, revision A, Gaussian Inc., Pittsburgh PA, 1992.
- 20 R. G. Snyder and J. H. Schachtschneider, *Spectrochim. Acta*, 1965, **21**, 165.
- 21 P. Pulay, J.-G. Lee and J. E. Boggs, *J. Chem. Phys.*, 1983, **79**, 3382.
- 22 R. Ditchfield and K. Seidman, *Chem. Phys. Lett.*, 1978, **54**, 57.
- 23 D. J. Defrees, B. A. Levi, S. K. Pollack, W. J. Hehre, J. S. Binkley and J. A. Pople, *J. Am. Chem. Soc.*, 1979, **101**, 4085.
- 24 R. G. Snyder, A. L. Aljibury, H. L. Strauss, H. L. Casal, K. M. Gough and W. F. Murphy, *J. Chem. Phys.*, 1984, **81**, 5352.
- 25 R. A. MacPhail and R. G. Snyder, *J. Chem. Phys.*, 1989, **91**, 3895.